Journal of Solid State Chemistry 182 (2009) 2918–2923

Contents lists available at ScienceDirect

Journal of Solid State Chemistry

journal homepage: www.elsevier.com/locate/jssc

Metal–organic coordination architectures of azole heterocycle ligands bearing acetic acid groups: Synthesis, structure and magnetic properties

Bo-Wen Hu, Jiong-Peng Zhao, Qian Yang, Tong-Liang Hu, Wen-Ping Du, Xian-He Bu*

Department of Chemistry, Nankai University, Tianjin 300071, China

ARTICLE INFO

Article history:
Received 15 March 2009
Received in revised form
13 July 2009
Accepted 26 July 2009
Available online 7 August 2009

Keywords:
Azole heterocycle ligands
Coordination architectures
Crystal structure
Magnetic properties

ABSTRACT

Four new coordination complexes with azole heterocycle ligands bearing acetic acid groups, $[Co(\mathbf{L^1})_2]_n$ (**1**), $[Cu\mathbf{L^1}N_3]_n$ (**2**), $[Cu(\mathbf{L^2})_2\cdot 0.5C_2H_5OH\cdot H_2O]_n$ (**3**) and $[Co(\mathbf{L^2})_2]_n$ (**4**) (here, $H\mathbf{L^1}$ = 1H-imidazole-1-yl-acetic acid, $H\mathbf{L^2}$ = 1H-benzimidazole-1-yl-acetic acid) have been synthesized and structurally characterized. Single-crystal structure analysis shows that **3** and **4** are 2D complexes with 4^4-sql topologies, while another 2D complex **1** has a $(4^3)_2(4^6)$-kgd topology. And **2** is a 3D complex composed dinuclear $\mu_{1,1}$-bridging azido Cu^{II} entities with distorted *rutile* topology. The magnetic properties of **1** and **2** have been studied.

1. Introduction

The design and synthesis of coordination architectures to obtain peculiar structures and potential applications such as microelectronics, porosity, magnetism, optoelectronics and catalysis have attracted intense attention in coordination chemistry and materials chemistry [1–3]. Recently, a great variety of new metal–organic coordination architectures using heterocyclic carboxylic acids as building block have been reported [4,5]. The heterocyclic carboxylic acids ligands containing N and O donors offer great potential for fine control over coordination architectures [6,7]. On the other hand, magnetism has become a hot topic in the past decades [8–11]. The motivity is not only to gain new materials, which could be applied in information storage and molecular switches, but also to investigate the magneto-structural correlations [9].

The selection of bridging ligands is very important since they have a great effect on the magnetic metal–organic framework structures. The building blocks with multi-oxgen and nitrogen atoms can coordinate with metal ions in different ways and result in distinct magnetic properties [10,11]. Ligands based on azole heterocycle and carboxylate groups should be good building blocks for the construction of magnetic coordination complexes.

In this work, azole heterocycle ligands bearing acetic acid groups: 1H-imidazole-1-yl-acetic acid ($H\mathbf{L^1}$), 1H-benzimidazole-1-yl-acetic acid ($H\mathbf{L^2}$), have been synthesized. The reactions of these ligands with Cu^{II} and Co^{II} ions lead to the formation of four 2D coordination polymers, $[Cu(\mathbf{L^2})_2\cdot 0.5C_2H_5OH\cdot H_2O]_n$ (**3**) and $[Co(\mathbf{L^2})_2]_n$ (**4**) with similar 4^4-sql toplogy, but $[Co(\mathbf{L^1})_2]_n$ (**1**) with different $(4^3)_2(4^6)$-kgd topology. A 3D complex of $[Cu\mathbf{L^1}N_3]_n$ (**2**) with *rutile* network, which shows strong ferromagnetic coupling.

2. Experimental section

2.1. Materials and general methods

All the reagents for synthesis were obtained commercially and used as received. Elemental analyses of C, H and N were performed on a Perkin–Elmer 240C analyzer. Ligands $H\mathbf{L^1}$ and $H\mathbf{L^2}$ were synthesized by reported procedure [12]. The FT-IR spectra were recorded from KBr pellets in the range 4000–400 cm^{-1} on a TENSOR 27 (Bruker) spectrometer. The X-ray powder diffraction (XRPD) was recorded on a Rigaku D/Max-2500 diffractometer at 40 kV, 100 mA for a Cu-target tube and a graphite monochromator. Simulation of the XRPD spectra was carried out by the single-crystal data and diffraction-crystal module of the mercury (Hg) program available free of charge via the Internet at http://www.iucr.org. Magnetic data were collected at Nankai University using crushed crystals of the sample on a Quantum Design MPMS XL-7 SQUID magnetometer.

* Corresponding author. Fax: +862 223 502 458.
E-mail address: buxh@nankai.edu.cn (X.-H. Bu).

0022-4596/$ - see front matter © 2009 Elsevier Inc. All rights reserved.
doi:10.1016/j.jssc.2009.07.059

2.2. Synthesis of complexes 1–4

2.2.1. $[Co(\mathbf{L^1})_2]_n$ (**1**)

The crystals of compound **1** was prepared by a hydrothermal reaction: a mixture of $Co(NO_3)_2 \cdot 6H_2O$ (0.1 mmol), H$\mathbf{L^1}$ (0.2 mmol) and NaOH/H_2O (2 mL, 0.1 M) in 15 mL H_2O was sealed in a Teflon-lined stainless steel vessel (25 mL), heated at 120 °C for 2 days under autogenous pressure, and then cooled to room temperature. Yield: ~25% based on Co^{II}. FT-IR (KBr pellet, cm^{-1}): 3405, 3152, 2921, 2075, 1592, 1513, 1448, 1402, 1319, 1293, 1237, 1200, 1113, 1092, 1042, 984, 942, 922, 833, 799, 766, 702, 656, 630, 579, 431. Anal. Calcd. for $C_{10}H_{10}CoN_4O_4$: C, 38.85; H, 3.26; N, 18.12. Found: C, 38.61; H, 3.55; N, 17.82.

2.2.2. $[Cu\mathbf{L^1}N_3]_n$ (**2**)

A buffer layer of ethanol/H_2O (10 mL, 1:1) was carefully layered over a solution (2 mL) of H$\mathbf{L^1}$ (0.05 mmol) and NaN_3 (0.05 mmol) in H_2O. Then a solution of $Cu(NO_3)_2$ (0.1 mmol) in ethanol (3 mL) was layered on the buffer layer. Green block crystals were collected after 1 week. Yield: ~20% based on Cu^{II}. FT-IR (KBr pellet, cm^{-1}): 3415, 2066, 1639, 1618, 1515, 1439, 1400, 1303, 1291, 1238, 1154, 1112, 1087,952, 881, 835, 797, 753, 716, 624, 483, 408. Anal. Calcd. for $C_5H_5CuN_5O_2 \cdot 0.5H_2O$: C, 25.06; H, 2.52; N, 29.22. Found: C, 25.15; H, 2.47; N, 29.61.

CAUTION: Azide complexes are potentially explosive. Only a small amount of the materials should be prepared, and it should be handled with care.

2.2.3. $[Cu(\mathbf{L^2})_2 \cdot 0.5C_2H_5OH \cdot H_2O]_n$ (**3**)

3 was obtained by the similar method as described for **2** except for using H$\mathbf{L^2}$ instead of H$\mathbf{L^1}$. Yield: ~30% based on Cu^{II}. FT-IR (KBr pellet, cm^{-1}): 3415, 3109, 1638, 1618, 1521, 1464, 1433, 1391, 1296, 1261, 1210, 1154, 985, 918, 880, 840, 794, 776, 746, 704, 624. Anal. Calcd. for $C_{76}H_{76}Cu_4N_{16}O_{22}$: C, 50.16; H, 4.21; N, 12.32. Found: C, 49.71; H, 4.31; N, 12.05.

2.2.4. $[Co(\mathbf{L^2})_2]_n$ (**4**)

4 was obtained by the similar method as described for **1** except for using H$\mathbf{L^2}$ instead of H$\mathbf{L^1}$. Yield: ~30% based on Co^{II}. FT-IR (KBr pellet, cm^{-1}): 3415, 3090, 2982, 1815, 1639, 1514, 1482, 1462, 1439, 1385, 1313, 1291, 1262, 1194, 1100, 1012, 977, 931, 920, 880, 855, 797, 774, 752, 717, 704, 622, 545, 498, 484. Anal. Calcd. for $C_{18}H_{12}CoN_4O_4$: C, 53.09; H, 2.97; N, 13.76. Found: C, 52.92; H, 2.98; N, 13.88.

2.3. X-ray data collection and structure determinations

Single-crystal X-ray diffraction measurements for **1–4** were carried out on a Bruker Smart 1000 CCD diffractometer equipped with a graphite crystal monochromator situated in the incident beam. The determinations of unit cell parameters and data collections were performed with Mo-$K\alpha$ radiation ($\lambda = 0.71073$ Å) and unit cell dimensions were obtained with least-squares refinements. The program SAINT (Bruker, *SAINT Software Reference Manual*, Madison, Wisconsin, 1998) was used for integration of the diffraction profiles and semi-empirical absorption corrections were applied using SADABS program (Bruker, *SADABS: Program for Empirical Absorption Correction of Area Detector Data*, Madison, Wisconsin, 1998). The structure was solved by direct methods using the SHELXS program of the SHELXTL package and refined with SHELXL (Sheldrick, G. M., *SHELXTL Version 6.1.* Program for Solution and Refinement of Crystal Structures, University of Göttingen, Germany, 1998). The final refinement was performed by full-matrix least-squares methods with anisotropic thermal parameters for non-hydrogen atoms on F^2. Crystallographic data (excluding structure factors) for **1–4** have also been deposited on the Cambridge Crystallographic Data Centre as supplementary publication (no. CCDC-688355–688358). Copies of the data can be obtained free of charge on application to CCDC, 12 Union Road, Cambridge CB21EZ, UK (fax: (+44) 1223-336-033; e-mail: deposit@ccdc.cam.ac.uk). Details of the X-ray crystal structure analysis of **1–4** are summarized in Table 1.

3. Results and discussion

The structures of the four compounds can be classified into three types. **3** and **4** are 2D complexes with 4^4-sql topology; **1** is a 2D complex with a (3,6)-connected net and **2** is a 3D complex with distorted *rutile* topology (see the Supporting Information Fig. 1S). Selected bond lengths and angles of **1–4** are given in Table 2.

3.1. Structure descriptions of complexes 1–4

3.1.1. $[Co(\mathbf{L^1})_2]_n$ (**1**)

Single-crystal structure analysis shows that **1** possesses a 2D structure. Co^{II} hexacoordinated in octahedral fashion by two nitrogen atoms of imidazole [Co(1)–N(2) = 2.1327(15) Å] and four oxygen atoms of carboxylate [Co(1)–O(1) = 2.1102(13) Å, Co(1)–O(2) = 2.2049(13) Å] from six distinct $\mathbf{L^1}$ ligands. The coordination

Table 1
Crystal data and structure refinement parameters for complexes **1–4**.

	1	**2**	**3**	**4**
Chemical formula	$C_{10}H_{10}CoN_4O_4$	$C_5H_5CuN_5O_2$	$C_{76}H_{76}Cu_4N_{16}O_{22}$	$C_{18}H_{12}CoN_4O_4$
Formula weight	309.15	230.68	1819.69	407.25
Space group	$P2_1/n$	$P2_1/n$	$P2_1/c$	$P2_1/n$
a (Å)	8.2873(16)	4.8922(10)	5.5016(11)	8.7414(17)
b (Å)	5.0188(10)	11.420(2)	15.343(3)	13.042(3)
c (Å)	12.307(3)	14.253(3)	24.415(5)	15.107(3)
β (deg.)	91.238(3)	90.02(3)	94.63(3)	97.99(3)
V (Å)	511.75(18)	796.3(3)	2054.1(7)	1705.6(6)
Z	2	4	1	4
D ($g\,cm^{-3}$)	2.006	1.924	1.471	1.586
μ (mm^{-1})	1.696	2.714	1.104	1.040
T (K)	294(2)	293(2)	293(2)	293(2)
R^a/wR^b	00230/0.0580	0.0556/0.1294	0.0924/0.2184	0.0369/0.0959

[a] $R = \Sigma(||F_o|-|F_c||)/\Sigma|F_o|$.
[b] $wR = [\Sigma[w(F_o^2-F_c^2)^2]/\Sigma w(F_o^2)^2]^{1/2}$.

angles vary from 85.06(5)° to 94.94(5)° (Fig. 1a and Table 2). The ligand $\mathbf{L^1}$ in **1** connected two Co^{II} ions *via* carboxylato bridge composing the Co/COO^- chains, which bonded *via* N of the imidazole ring to form a 2D layer (Fig. 1b) with $(4^3)_2(4^6)$-kgd topological net [13].

3.1.2. $[Cu\mathbf{L^1}N_3]_n$ (**2**)

Cu^{II} ion in **2** has a slightly distorted five-coordinated square-based pyramid (CuO_2N_3). The apical position of Cu^{II} is occupied by an O atom of the carboxylate [Cu(1)–O(2) = 2.289(3) Å], and the equatorial plane is formed by an O atom of the carboxylato [Cu(1)–O(1) = 1.964(3) Å], two equivalent N atoms of two $\mu_{1,1}$-bridging azides [Cu(1)–N(1) = 2.003(3) Å; Cu(1)–N(1A) = 2.006(4) Å], and one N atom from imidazole ring [Cu(1)–N(4) = 1.988(3) Å]. First, double end-on (EO) azides link two Cu^{II} ions to form a dinuclear Cu^{II} entity (Fig. 2a), in which the Cu(1)–N(1)–Cu(1A) angle is 101.24(16)°. Second, these dinuclear entities form a 1D chain through an *anti-syn* carboxylato bridging group of $\mathbf{L^1}$. Finally, these chains are connected *via* the imidazole group of the $\mathbf{L^1}$ ligands (μ–N,O,O bridging mode) to form the 3D structure (Fig. 2b). If the dinuclear Cu^{II} entity is treated as a 6-connected node and the $\mathbf{L^1}$ ligand as a 3-connected node, the network of **2** can be described as a distorted infinite 3D 3,6-conn $(4\cdot6^2)_2(4^2\cdot6^{10}\cdot8^3)$-rtl network.

Table 2
Selected bond distances (Å) and angles (deg.) for complexes **1–4.**

$[Co(L^1)2]_n$ (1)			
Co(1)–O(2)$^{\#1}$	2.2049(13)	Co(1)–O(1)$^{\#2}$	2.1102(13)
Co(1)–N(2)$^{\#3}$	2.1327(15)		
O(1)$^{\#2}$–Co(1)–N(2)$^{\#3}$	93.40(6)	O(1)–Co(1)–N(2)$^{\#3}$	86.60(6)
N(2)$^{\#3}$–Co(1)–O(2)$^{\#4}$	85.06(5)	N(2)$^{\#4}$–Co(1)–O(2)$^{\#5}$	94.94(5)
$[CuL^1N_3]_n$ (2)			
Cu(1)–O(1)$^{\#1}$	1.964(3)	Cu(1)–N(4)	1.988(3)
Cu(1)–N(1)	2.003(3)	Cu(1)–N(1)$^{\#2}$	2.006(4)
Cu(1)–O(2)$^{\#3}$	2.289(3)		
O(1)$^{\#1}$–Cu(1)–N(1)	90.33(14)	N(4)–Cu(1)–N(1)$^{\#2}$	94.38(14)
N(1)–Cu(1)–N(1)$^{\#2}$	78.76(16)	N(4)–Cu(1)–O(2)$^{\#3}$	88.94(12)
N(1)–Cu(1)–O(2)$^{\#3}$	94.79(15)		
$[Cu(L^2)_2\cdot0.5C_2H_5OH\cdot H_2O]_n$ (3)			
Cu(1)–O(4)$^{\#1}$	1.975(5)	Cu(1)–O(2)$^{\#2}$	1.987(5)
Cu(1)–N(3)	1.993(6)	Cu(1)–N(1)	2.005(6)
O(4)$^{\#1}$–Cu(1)–O(2)$^{\#2}$	87.2(2)	O(2)$^{\#2}$–Cu(1)–N(3)	88.8(2)
O(4)$^{\#1}$–Cu(1)–N(1)	88.7(2)	N(3)–Cu(1)–N(1)	95.8(2)
$[Co(L^2)2]_n$ (4)			
Co(1)–O(1)$^{\#1}$	1.928(2)	Co(1)–O(4)	1.943(2)
Co(1)–N(2)	2.006(3)	Co(1)–N(3)	2.009(2)
O(1)$^{\#1}$–Co(1)–O(4)	99.24(11)	O(1)$^{\#1}$–Co(1)–N(2)	122.18(11)
O(4)–Co(1)–N(2)	115.32(10)	O(1)$^{\#1}$–Co(1)–N(3)	112.32(11)
O(4)–Co(1)–N(3)	103.78(9)	N(2)–Co(1)–N(3)	102.95(10)

Symmetry mode: For **1**, #1, *x*, *y*−1, *z*; #2−*x*, −*y*−1, −*z*+2; #3 *x*−1/2, −*y*−1/2, *z*+1/2, #4 −*x*+1/2, *y*−1/2, −*z*+3/2; #5 −*x*, −*y*, −*z*+2. For **2**, #1, −*x*+1/2, *y*−1/2, −*z*+3/2; #2, −*x*+1, −*y*, −*z*+1; #3, −*x*+3/2, *y*−1/2, −*z*+3/2. For **3**, #1, −*x*+1, *y*+1/2, −*z*+1/2; #2, −*x*+2, *y*−1/2, −*z*+1/2. For **4**, #1, −*x*+1/2, *y*+1/2, −*z*+1/2.

3.1.3. $[Cu(\mathbf{L^2})_2\cdot0.5C_2H_5OH\cdot H_2O]_n$ (**3**)

One kind of ligand $\mathbf{L^2}$ in **3** connects two Cu^{II} ion *via* one O atom of the carboxylate and N atom of of the imidazole ring [Cu(1)–O(2) = 1.987(5) Å, Cu(1)–N(1) = 2.005(6) Å]. The other kind of ligand $\mathbf{L^2}$ connects two Cu^{II} ion in different bond lengths [Cu(1)–O(4) = 1.975(5) Å, Cu(1)–N(3) = 1.993(6) Å]. Cu^{II} ions of **3** with four coordinated square bonded by ligand $\mathbf{L^2}$ form 2D networks, which is similar with 2D structure of **2,** but with 4^4-sql (Fig. 3). All the 2D layers in **3** are parallel to each other in the crystal packing like AAAA 4^4-sql.

3.1.4. $[Co(\mathbf{L^2})_2]_n$ (**4**)

Co^{II} ion of **4** has a slight distorted tetrahedral coordination geometry comprised of two O donors and two N donors from four distinct $\mathbf{L^2}$ ligands with Co–O bond lengths of 1.928(2) and 1.943(2) Å, Co–N bond lengths of 2.006(3) and 2.009(2) Å, and the bond angles around the Co^{II} center range from 99.24(11)° to 122.18(11)°. $\mathbf{L^2}$ ligands acts as μ_2-bridge in such a way that O1 of carboxylate coordinates to one Co^{II} centers and N2 of imidazole coordinate to another Co^{II} ions. The Co^{II} ions are interconnected by four $\mathbf{L^2}$ ligands to form a zig–zag 2D layer (Fig. 4) with similar 4^4-sql topology of **3** but different in the crystal packing. All the 2D layers in **4** are parallel to each other as ABAB 4^4-sql.

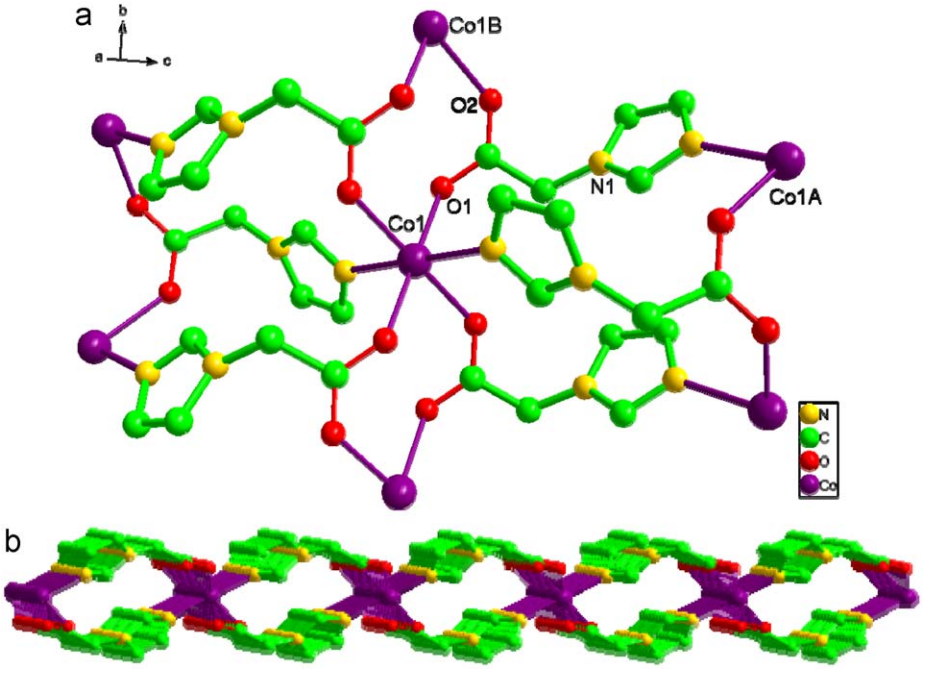

Fig. 1. (a) The coordination environment of the Co^{II} center in **1** (symmetry code: **A** *x*, 1+*y*, *z*; **B** 1/2−*x*, 3/2+*y*, 3/2−*z*), (b) the 2D network of **1**, viewed from the *b*-axis.

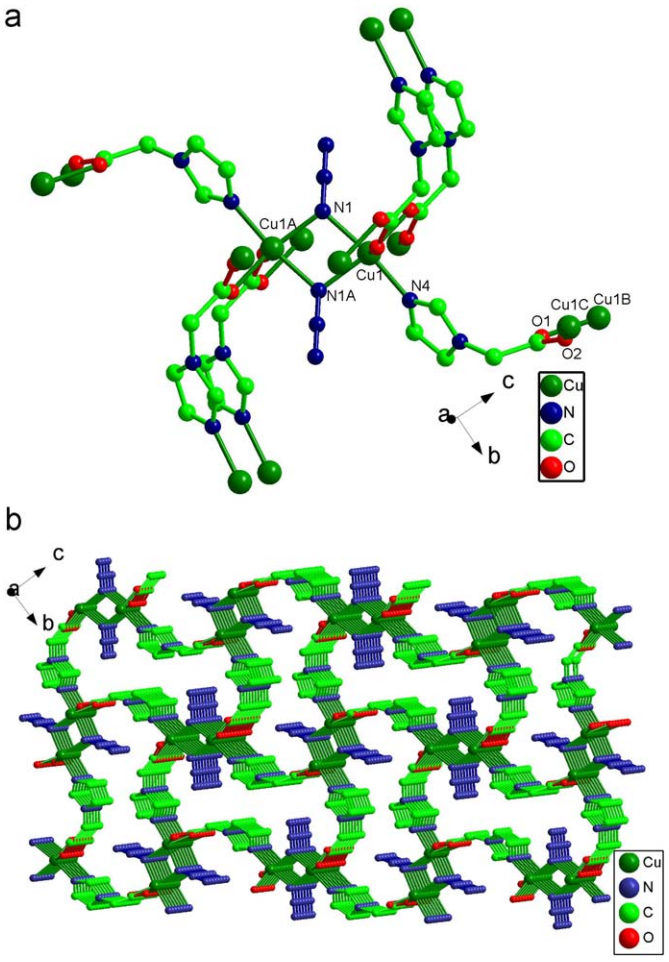

Fig. 2. (a) The coordination environment of the Cu^{II} center in **2** (symmetry code: **A** $1-x, -y, 1-z$; **B** $1/2-x, 1/2+y, 3/2-z$; **C** $3/2-x, 1/2+y, 3/2-z$) and (b) the 3D network of **2**.

A comparison of the structures of complexes **1**–**4**, we may find many differences among these compounds, which may be attributed to the steric effect and different coordination modes of the ligands. The terminal group of ligands was changed from imidazole to benzoimidazole, resulting in distinct 2D layers for the same metal ions. Complexes **1, 3** and **4** have different 2D networks and complex **3** has a 3D framework. Because of the

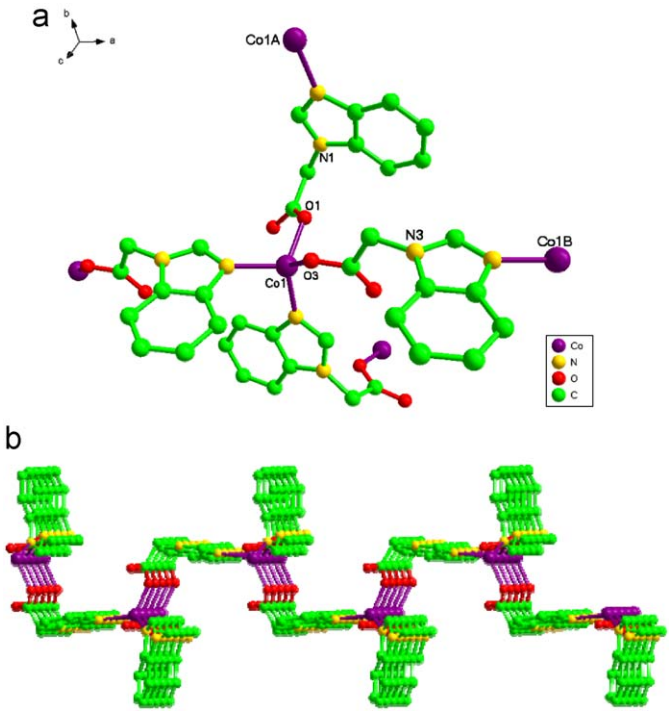

Fig. 4. (a) The coordination environment of the Co^{II} center in **4** (symmetry code: **A** $1/2-x, 1/2+y, 1/2-z$; **B** $1+x, y, z$) and (b) the 2D network of **4**.

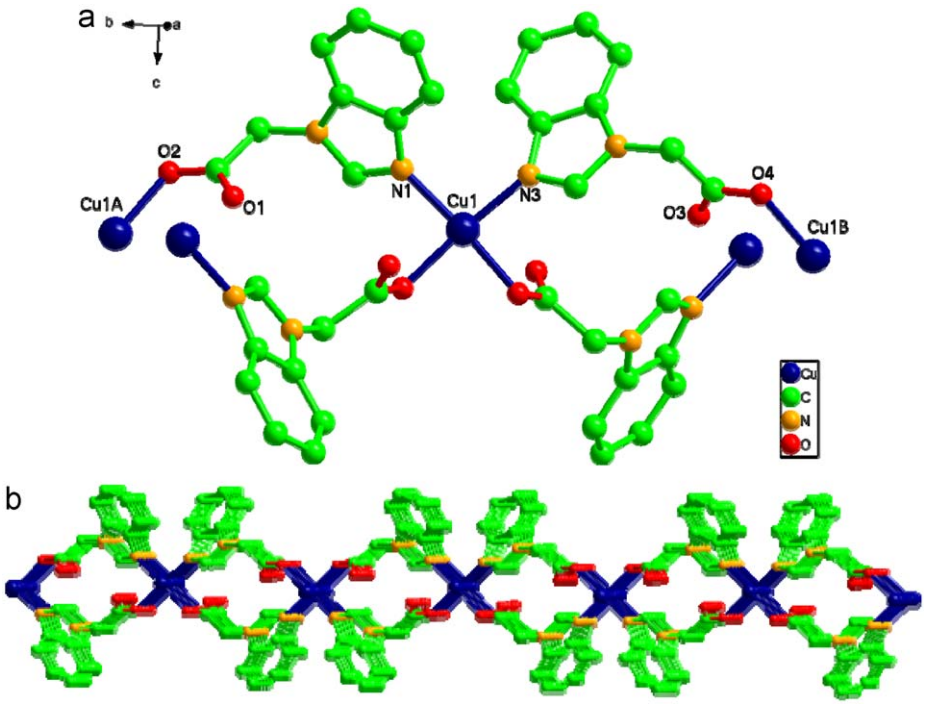

Fig. 3. (a) The coordination environment of the Cu^{II} center in **3** (symmetry code: **A** $-1+x, y, z$; **B** $x, -1+y, z$) and (b) the 2D network of **3**.

steric hindrance of benzimidazole ring from $\mathbf{L^2}$, octahedral Co^{II} ions in **1** form rare $(4^3)_2(4^6)$-kgd topology and tetrahedral coordinated Co^{II} ions in **4** resulted in zig–zag 2D layers with 4^4-sql. While in the 3D complex **2**, when the azides introduced as the second ligand, double end-on azides bridge dinuclear Cu^{II} entities bond by $\mathbf{L^1}$ ligands to form 3D distorted *rutile* topology. Unfortunately, single crystal of complex with both $\mathbf{L^2}$ ligand and azide is not obtained. Above all, introduction of the rigid ligand or the second ligand have a great influence on the structures of such coordination complexes and their properties.

3.2. XRPD results

In order to confirm the phase purity of the bulk materials, X-ray powder diffraction (XRPD) experiments were carried out for complexes **1**–**4**. The experimental and computer-simulated patterns of **1**–**4** are shown in Fig. 2S (see the Supporting Information). Although the experimental patterns have a few un-indexed diffraction lines and some are slightly broadened in comparison with those simulated from the single-crystal models, it still can be well considered that the bulk synthesized materials and the as-grown crystals are homogeneous for complexes **1**–**4**.

3.3. Magnetic properties

Magnetic properties data were collected for a crushed crystalline sample of complexes **1** and **2**. For complexes **3** and **4**, metal ions are connected by long bridging ligands, which usually gives very weak antiferromagnetic interactions [14], therefore we did not study the magnetic behavior.

3.3.1. Magnetic properties of *1*

The temperature dependence of the magnetic susceptibility in 2 to 300 K temperature range under 1000 Oe and the magnetization dependence with field at 2 K for **1** are shown in Fig. 5. At 300 K, $\chi_m T$ (3.29 $cm^3\,mol^{-1}\,K$) corresponds to what is expected for Co^{II} ions with spin–orbit coupling [15]. As T is lowered, $\chi_m T$ decreases smoothly and reaches a rounded minimum around 23 K with $\chi_m T = 2.38\ cm^3\,mol^{-1}\,K$, and then increases as T is lowered further. Such behavior is characteristic of 2D ferrimagnetism. Although this decrease of $\chi_m T$ was due to the spin–orbit coupling effect of the octahedral Co^{II} ion [16], it is strong enough to confirm the presence of antiferromagnetic coupling between chains [17]. As T is lowered further below the minimum of $\chi_m T$, the correlation intrachain increases rapidly. The reduced molar magnetization at 2 K is shown in Fig. 5 inset. The maximum value of $M/N\beta$ reached at 5 T is well below the expected value of 2.5 for Co^{II} ions with $g = 2.2$ and $S = 3/2$, indicating ferromagnetic coupling between Co^{II} ions through carboxylato bridges at this temperature.

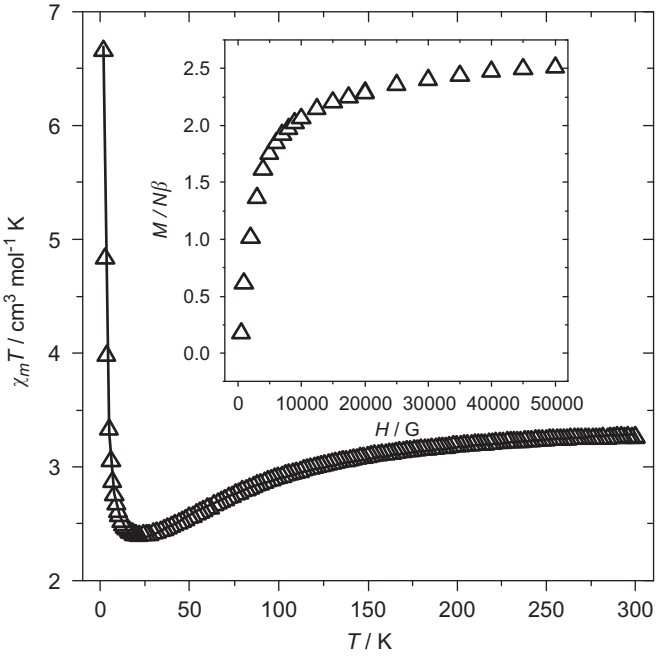

Fig. 5. $\chi_m T$ vs T plot for **1**. Inset: field dependence of the magnetization for **1**.

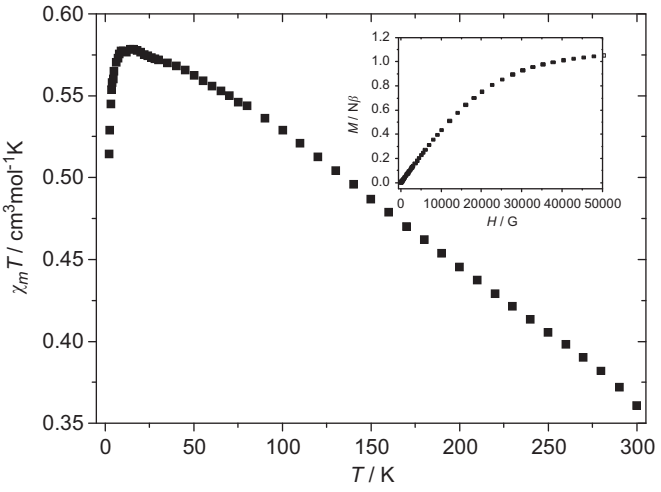

Fig. 6. $\chi_m T$ vs T plot for **2**. Inset: field dependence of the magnetization for **2**.

3.3.2. Magnetic properties of *2*

Magnetic susceptibility data were collected for **2** in the 2–300 K temperature range at applied *dc* fields of 2000 Oe. The magnetic properties of **2** as $\chi_m T$ vs T plot (χ_m is the molar magnetic susceptibility for two Cu^{II} ions) and the reduced magnetization ($M/N\beta$ vs H) are shown in Fig. 6. The value of $\chi_m T$ at 300 K is 0.36 $cm^3\,mol^{-1}\,K$. Starting from room temperature, $\chi_m T$ values increase to 0.58 $cm^3\,mol^{-1}\,K$ at 14 K and below 14 K, they decrease quickly to 0.51 $cm^3\,mol^{-1}\,K$ at 2 K. This feature is characteristic of strong intradimer, $[Cu_2]$, ferromagnetic coupling with weak interdimer and interchains antiferromagnetic interactions. The reduced molar magnetization at 2 K (Fig. 6 inset) corroborates the ferromagnetic coupling: the $M/N\beta$ value at 5 T is close to 1.1 $N\beta$. **2** is considered as formed by dinuclear entities [18], linked among them through *anti-syn* carboxylato leading to weak magnetic coupling at apical–equatorial positions and through the $\mathbf{L^1}$ ligands, which also mediates weak coupling. The strong ferromagnetic coupling can be interpreted as a consequence of the existence of the two azido bridges in end-on coordination mode, which gives ferromagnetic coupling [10e].

4. Conclusion

In summary, four new coordination compounds with azole heterocycle ligands bearing acetic acid groups were synthesized and structurally characterized. The structural comparison of **1**–**4** indicates that the terminal groups of the ligands affect the coordination modes of metal ions and thereby the topology networks of such complexes. And complexes **1** and **2** showed ferromagnetic couplings.

Acknowledgments

This work was supported by the National Natural Science Foundation of China (50673043, 20531040 and 20773068), the 973 Program of China (2007CB815305) and the Natural Science Fund of Tianjin, China (07 JCZDJC00500).

Appendix A. Supplementary material

Supplementary data associated with this article can be found in the online version at doi:10.1016/jssc.2009.07.059.

References

[1] B. Zhang, X.C. Ye, C.M. Wang, Y. Xie, J. Mater. Chem. 17 (2007) 2706–2712;
K.X. Huang, Y.L. Song, Z.R. Pan, Y.Z. Li, X. Zhuo, H.G. Zheng, Inorg. Chem. 46 (2007) 6233–6235;
O.K. Farha, A.M. Spokoyny, K.L. Mulfort, M.F. Hawthorne, C.A. Mirkin, J.T. Hupp, J. Am. Chem. Soc. 129 (2007) 12680–12681;
S. Hasegawa, S. Horike, R. Matsuda, S. Furukawa, K. Mochizuki, Y. Kinoshita, S. Kitagawa, J. Am. Chem. Soc. 129 (2007) 2607–2614.

[2] O.M. Yaghi, M. O'Keeffe, N.W. Ockwig, H.K. Chae, M. Eddaoudi, J. Kim, Nature 423 (2003) 705–714;
C.-H. Li, K.-L. Huang, J.-M. Dou, Y.-N. Chi, Y.-Q. Xu, L. Shen, D.-Q. Wang, C.-W. Hu, Cryst. Growth Des. 8 (2008) 3141–3143;
M. Murugesu, S. Takahashi, A. Wilson, K.A. Abboud, W. Wernsdorfer, S. Hill, G. Christou, Inorg. Chem. 47 (2008) 9459–9470;
J.-R. Li, Y. Tao, Q. Yu, X.-H. Bu, H. Sakamoto, S. Kitagawa, Chem. Eur. J. 14 (2008) 2771–2776.

[3] B. Moulton, M.J. Zaworotko, Chem. Rev. 101 (2001) 1629–1658;
O.R. Evans, W. Lin, Acc. Chem. Res. 35 (2002) 511–522;
X.-H. Bu, M.-L. Tong, H.-C. Chang, S. Kitagawa, S.R. Batten, Angew. Chem. Int. Ed. 43 (2004) 192–195;
H. Yang, J. Lin, J. Chen, X. Zhu, S. Gao, R. Cao, Cryst. Growth Des. 8 (2004) 2623–2625;
W. Ki, J. Li, J. Am. Chem. Soc. 130 (2008) 8114–8115.

[4] Y. Akhriff, J. Server-Carrio, A. Sancho, J. Garcia-Lozano, E. Escriva, J.V. Folgado, L. Soto, Inorg. Chem. 38 (1999) 1174–1185;
G. Lemercier, E. Mulliez, C. Brouca-Cabarrecq, F. Dahan, J. Tuchagues, Inorg. Chem. 43 (2004) 2105–2113;
R. Ivanikova, R. Boca, L. Dlhan, H. Fuess, A. Maslejova, V. Mrazova, I. Svoboda, J. Titis, Polyhedron 25 (2006) 3261–3268;
G. Beobide, O. Castillo, A. Luque, U. Garcia-Couceiro, J.P. Garcia-Teran, P. Roman, Inorg. Chem. 45 (2006) 5367–5382;
J.-R. Li, Q. Yu, Y. Tao, X.-H. Bu, J. Ribas, S.R. Batten, Chem. Commun. (2007) 2290–2292.

[5] E.Y. Lee, M.P. Suh, Angew. Chem. Int. Ed. 43 (2004) 2798–2801;
Z. Fei, T.J. Geldbach, D. Zhao, R. Scopelliti, P.J. Dyson, Inorg. Chem. 44 (2005) 5200–5202;
R. Baldoma, M. Monfort, J. Ribas, X. Solans, M.A. Maestro, Inorg. Chem. 45 (2006) 8144–8155;
W.-G. Lu, J.-Z. Gu, L. Jiang, M.-Y. Tan, T.-B. Lu, Cryst. Growth Des. 8 (2008) 192–199.

[6] X.-M. Zhang, M.-L. Tong, X.-M. Chen, Angew. Chem. Int. Ed. 41 (2002) 1029–1031;
D.M. Ciurtin, M.D. Smith, H.C. zur Loye, Chem. Commun. (2002) 74–75;
D.M. Ciurtin, M.D. Smith, H.C. zur Loye, Dalton Trans. (2003) 1245–1250;
J.-Y. Lu, Coord. Chem. Rev. 246 (2003) 327–347;
S.M. Humphrey, P.T. Wood, J. Am. Chem. Soc. 126 (2004) 13236–13237;
S.K. Ghosh, P.K. Bharadwaj, Inorg. Chem. 44 (2005) 3156–3161.

[7] J. Fan, W.-Y. Sun, T. Okamura, Y.-Q. Zheng, B. Sui, W.-X. Tang, N. Ueyama, Cryst. Growth Des. 4 (2004) 579–584;
C.-Y. Sun, X.-J. Zheng, S. Gao, L.-C. Li, L.-P. Jin, Eur. J. Inorg. Chem. (2005) 4150–4159;
J.F. Eubank, R.D. Walsh, M. Eddaoudi, Chem. Commun. (2005) 2095–2097;
M.-B. Zhang, J. Zhang, S.T. Zheng, G.-Y. Yang, Angew. Chem. Int. Ed. 44 (2005) 1385–1388;
Y.-T. Wang, G.-M. Tang, Y. Wu, X.-Y. Qin, D.-W. Qin, J. Mol. Struct. 831 (2007) 61–68;
P. Mahata, K.V. Ramya, S. Natarajan, Chem. Eur. J 14 (2008) 5839–5850.

[8] T. Kajiwara, A. Kamiyama, T. Ito, Chem. Commun. (2002) 1256–1257;
J.R. Galán-Mascarós, K.R. Dunbar, Angew. Chem. Int. Ed. 42 (2003) 2289–2293;
D. Maspoch, D. Ruiz-Molina, K. Wurst, N. Domingo, M. Cavallini, F. Biscarini, J. Tejada, C. Rovira, J. Veciana, Nat. Mater. 2 (2003) 190–195;
D. Maspoch, D. Ruiz-Molina, J. Veciana, J. Mater. Chem. 14 (2004) 2713–2723;
R.D. Poulsen, A. Bentien, M. Chevalier, B.B. Iversen, J. Am. Chem. Soc. 127 (2005) 9156–9166;
N. Motokawa, H. Miyasaka, M. Yamashita, K.R. Dunbar, Angew. Chem. Int. Ed. 47 (2008) 7760–7763.

[9] Y. Suzuki, M. Fujimori, H. Yoshikawa, K. Awaga, Chem. Eur. J. 10 (2004) 5158–5164;
V. Zeleňák, A. Orendáčová, I. Císařová, J. Černák, O.V. Kravchyna, J.H. Park, M. Orendáč, A.G. Anders, A. Feher, M.W. Meisel, Inorg. Chem. 45 (2006) 1774–1782;
U. García-Couceiro, O. Castillo, A. Luque, J.P. Garcíá-Terán, G. Beobide, P. Román, Cryst. Growth Des. 6 (2006) 1839–1847;
J.-R. Li, Q. Yu, E.C. Sañudo, Y. Tao, W.-C. Song, X.-H. Bu, Chem. Mater. 20 (2008) 1218–1220.

[10] J. Ribas-Ariño, J.J. Novoa, J.S. Miller, J. Mater. Chem. 16 (2006) 2600–2611;
V.I. Ovcharenko, E.V. Gorelik, S.V. Fokin, G.V. Romanenko, V.N. Ikorskii, A.V. Krashilina, V.K. Cherkasov, G.A. Abakumov, J. Am. Chem. Soc. 129 (2007) 10512–10521;
F. Pan, Z.-M. Wang, S. Gao, Inorg. Chem. 46 (2007) 10221–10228;
Y.-F. Yue, B.-W. Wang, E.-Q. Gao, Ch.-J. Fang, C. He, C.-H. Yan, Chem. Commun. (2007) 2034–2036;
Y.-F. Zeng, X. Hu, F.-C. Liu, X.-H. Bu, Chem. Soc. Rev. 38 (2009) 469–480.

[11] J. Tercero, C. Diaz, J. Ribas, E. Ruiz, J. Mahía, M. Maestro, Inorg. Chem. 41 (2002) 6780–6789;
C.N.R. Rao, S. Natarajan, R. Vaidhyanathan, Angew. Chem. Int. Ed. 43 (2004) 1466–1496;
K.S. Min, A.L. Rhinegold, J.S. Miller, Inorg. Chem. 44 (2005) 8433–8441;
H.B. Xu, Z.M. Wang, T. Liu, S. Gao, Inorg. Chem. 46 (2007) 3089–3096;
J.-Y. Zhang, Y. Ma, A.-L. Cheng, Q. Yue, Q. Sun, E.-Q. Gao, Dalton Trans. (2008) 2061–2066.

[12] T.-L. Hu, W.-P. Du, B.-W. Hu, J.-R. Li, X.-H. Bu, R. Cao, Cryst. Eng. Commun. 10 (2008) 1037–1043.

[13] Q.-J. Deng, M.-C. Wu, Z.-T. Liu, M.-H. Zeng, J.-Y. Huang, H. Liang, J. Mol. Struct. 876 (2008) 162–169;
Y.-Q. Lan, S.-L. Li, J.-S. Qin, D.-Y. Du, X.-L. Wang, Z.-M. Su, Q. Fu, Inorg. Chem. 47 (2008) 10600–10610.

[14] S.C. Manna, S. Konar, E. Zangrando, K. Okamoto, J. Ribas, N.R. Chaudhuri, Eur. J. Inorg. Chem. (2005) 4646–4654;
S.C. Manna, E. Zangrando, J. Ribas, N.R. Chaudhuri, Dalton Trans. (2007) 1383–1391.

[15] O. Kahn, in: Molecular Magnetism, VCH, New York, 1993.

[16] P.J. van Koningsbruggen, O. Kahn, K. Nakatani, Y. Pei, J.P. Renard, M. Drillon, P. Legoll, Inorg. Chem. 29 (1990) 3325–3331.

[17] C.L.M. Pereira, A.C. Doriguetto, C. Konzen, L.C. Meira-Belo, U.A. Leitão, N.G. Fernandes, Y.P. Mascarenhas, J. Ellena, A.L. Brandl, M. Knobel, H.O. Stumpf, Eur. J. Inorg. Chem. (2005) 5018–5025.

[18] E. Ruiz, J. Cano, S. Alvarez, P. Alemany, J. Am. Chem. Soc. 120 (1998) 11122–11129;
F.-C. Liu, Y.-F Zeng, J.-P. Zhao, B.-W. Hu, E.C. Sañudo, J. Ribas, X.-H. Bu, Inorg. Chem. 46 (2007) 7698–7700.